Optical and Quantum Electronics **10** (*1978*) *301–309*

Wave propagation in a single-mode fibre with dip in the refractive index

W. A. GAMBLING, H. MATSUMURA, CATHERINE M. RAGDALE
Department of Electronics, University of Southampton, Southampton, England

Received 3 January 1978

A theoretical study has been carried out on propagation in single-mode fibres having a dip in the refractive index at the centre of the core. The energy of the mode gradually spreads from the centre of the core with increase of the degree of the dip. Nevertheless the near- and far-field distributions of such single-mode fibres are very nearly Gaussian in shape. A simple method of estimating the limit of the single-mode region for any kind of index profile is presented. For a particular class of profiles, dip widths up to 30% have a negligible effect on the propagation characteristics.

1. Introduction

A particular virtue of the homogeneous chemical vapour deposition method is that it greatly simplifies the fabrication of single-mode fibres [1]. However, it is difficult to produce a perfectly-stepped refractive-index distribution because of diffusion at the core–cladding boundary, the effect of which on the propagation of the HE_{11}-mode has been discussed elsewhere [2, 3]. However, a more serious problem will result from the dip in refractive index at the centre of the core which occurs due to the preferential evaporation of the more volatile component during the preform collapsing stage.

Stolen [4] has considered this problem especially in the multimode region by using the stepped ring profile. We have also studied the tolerance of the dip on the propagation of the HE_{11}-mode by calculating the cut-off frequency of the second mode [5]. However, as far as we know, a theoretical study on the propagation of the HE_{11}-mode in a single-mode fibre with a dip in the core centre has not been reported so far. On the experimental side, most of the research work using single-mode fibres, for example the determination of fibre diameter $2a$, normalized frequency V and fibre numerical aperture by using the far-field pattern [6], is based on the theory of a perfect step-index fibre.

In order to assess the applicability of the theory, the propagation characteristics of the distorted fibre have to be analysed. We study, therefore, the propagation of the HE_{11}-mode in a single-mode fibre having a dip in the refractive index. The most important factor in a single-mode fibre, regardless of the index distribution, whether step-index, graded-index and so on, is the spot size of the HE_{11}-mode [7–9]. Therefore, the particular interest of this study is to determine the change of mode spot size as a function of the degree of dip. We limit our discussion to weakly-guiding fibres defined by

$$\Delta = \frac{n_1^2 - n_2^2}{2n_1^2} \approx \frac{n_1 - n_2}{n_1} \ll 1 \tag{1}$$

where Δ is the relative index difference between core and cladding, and n_1 and n_2 are the maximum values of the refractive index of the fibre core and of the cladding, respectively.

2. Field distribution and the characteristic equation

The dip is represented by a radial, r, variation of dielectric constant in a fibre core, diameter $2a$, given by:

$$\begin{aligned} \epsilon(R) &= \epsilon_1[1 - 2\delta(1-R)^\alpha] \qquad 0 \leqslant R \leqslant 1 \\ &= \epsilon_1(1 - 2\Delta) = \epsilon_2 = n_2^2 \quad 1 \leqslant R \end{aligned} \tag{2}$$

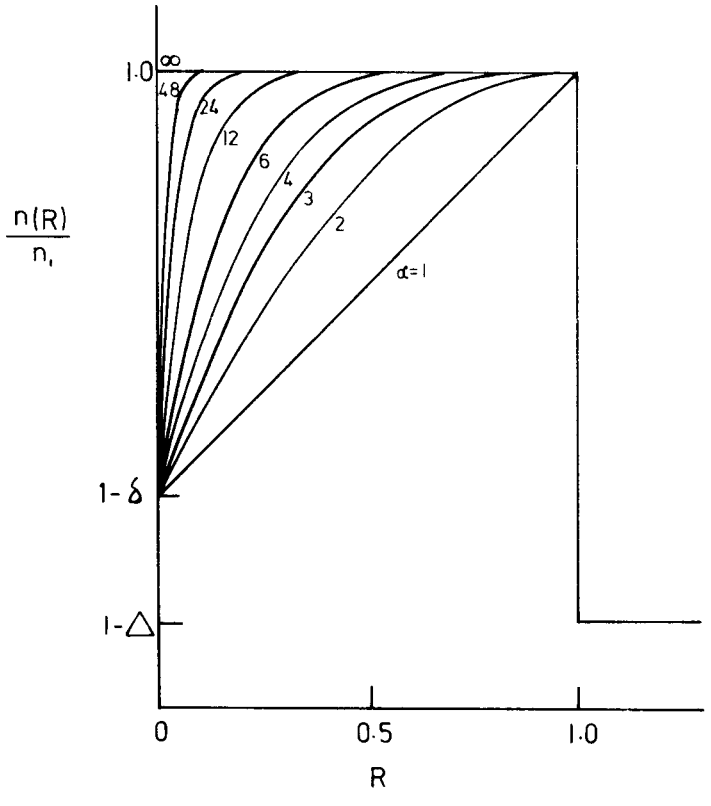

Figure 1 Refractive-index profile as a function of normalized radius for various values of α.

where $R = r/a$, $\epsilon_1 = n_1^2$ is the dielectric constant at the edge of the core, δ is the relative difference in dielectric constant between the edge and the centre of the core and denotes the dip depth, and α is a parameter between 1 and ∞ which defines the dip width. The resulting profile distributions are shown in Fig. 1.

The guided modes of a weakly-guiding fibre are very nearly transverse and linearly polarized (LP-modes). Thus the electric and magnetic fields of the HE_{11}-modes in terms of the cylindrical coordinates (r, θ, z) are given by

$$\begin{aligned} E_y &= AF(R) \\ H_x &= -n_1\left(\frac{\epsilon_0}{\mu_0}\right)^{1/2} AF(R) \\ E_z &= -\frac{j}{\beta a} A \frac{\mathrm{d}F(R)}{\mathrm{d}R} \sin\theta \\ H_z &= \frac{j}{ka}\left(\frac{\epsilon_0}{\mu_0}\right)^{1/2} A \frac{\mathrm{d}F}{\mathrm{d}R} \cos\theta \end{aligned} \qquad \text{in the core } (R \leqslant 1) \tag{3}$$

and

$$\begin{aligned} E_y &= A \frac{F(R=1)}{K_0(W)} K_0(WR) \\ H_x &= -n_1\left(\frac{\epsilon_0}{\mu_0}\right)^{1/2} A \frac{F(R=1)}{K_0(W)} K_0(WR) \\ E_z &= \frac{jW}{\beta a} A \frac{F(R=1)}{K_0(W)} K_1(WR) \sin\theta \end{aligned} \qquad \text{in the cladding } (R \geqslant 1)$$

$$H_z = -\frac{jW}{ka}\left(\frac{\epsilon_0}{\mu_0}\right)^{1/2} A \frac{F(R=1)}{K_0(W)} K_1(WR)\cos\theta$$

where ϵ_0 and μ_0 are the dielectric permittivity and magnetic permeability of vacuum, k the wavenumber in free space, and the time and z-variation $\exp[j(\omega t - \beta z)]$ is understood. $K_0(W)$ is the modified Hankel function and the function $F(R)$ is expressed by the scalar wave equation

$$\frac{d^2F(R)}{dR^2} + \frac{1}{R}\frac{dF(R)}{dR} + [U^2 - \gamma V^2(1-R)^\alpha]F(R) = 0 \tag{4}$$

where parameters U and W can be defined as

$$U^2 = (kn_1a)^2 - (\beta a)^2$$

and

$$W^2 = (\beta a)^2 - (kn_2a)^2.$$

The normalized frequency V is, therefore, given by

$$V^2 = U^2 + W^2 = (ka)^2(n_1^2 - n_2^2). \tag{6}$$

γ in Equation 4 is the normalized depth of the dip at the centre of the core;

$$\gamma = \delta/\Delta. \tag{7}$$

The amplitude coefficient A is given by

$$A^2 = \frac{(\mu_0/E_0)^{1/2}}{2\pi n_1 a^2\left\{\int_0^1 F^2(R)R\,dR + \frac{F^2(R=1)}{2}\left[\frac{K_1^2(W)}{K_0^2(W)} - 1\right]\right\}} \tag{8}$$

so as to normalize the total power to unity.

From the boundary condition that the electric field and its derivative are continuous at the boundary ($R = 1$), the eigenvalue equation is written as

$$\frac{1}{F(R)}\frac{dF(R)}{dR}\bigg|_{R=1} + \frac{WK_1(W)}{K_0(W)} = 0. \tag{9}$$

3. Eigenvalue as a function of α

The scalar equation (Equation 4) can be solved by the series expansion method. We set up a series in the interval $0 \leqslant R < 1$

$$F(R) = \sum_{n=0}^{\infty} a_n R^n \tag{10}$$

where $a_0 = 1$. Substituting this into Equation 4 and then equating coefficients of each power of R to zero, a series of equations for determination of the coefficients a_n in the series for the solution can be obtained.

By solving Equation 9 numerically, U–V curves are obtained for various index profiles (Figs. 2a and b). These show that the eigenvalue U increases considerably with increase in the degree of dip. In the extreme case where the doped ions in the centre of the fibre completely evaporate (i.e. $\gamma = 1$), differences of 29% and 18% from the U-value of the step-index fibre arise for $\alpha = 1$ and 2, respectively. The U-value approaches asymptotically that of the step-index fibre with increase of α. It is important to note that for $\alpha \geqslant 20$, the maximum deviation is only 0.6%. It may, therefore, be concluded that a fibre with a dip of $\alpha \geqslant 20$ behaves almost identically to the step-index fibre.

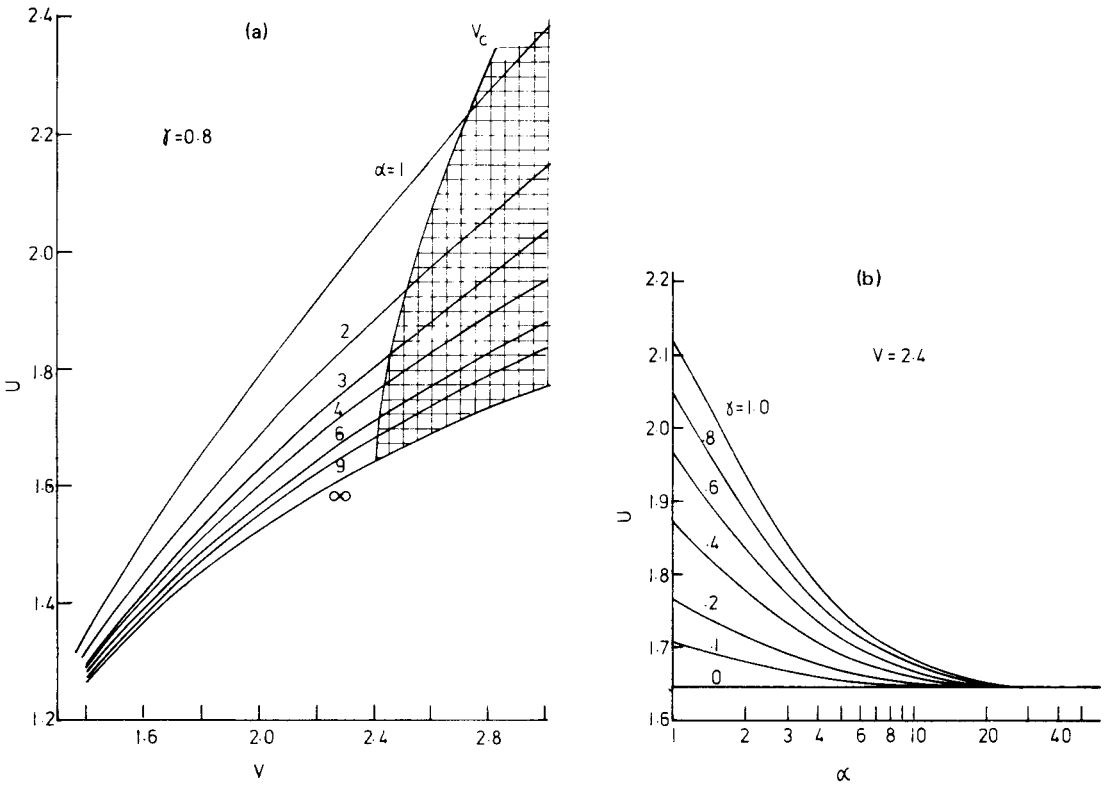

Figure 2 (a) Normalized frequency V versus eigenvalue U of HE_{11}-mode for various index profiles α at relative depth $\gamma = 0.8$. Shaded area shows the multimode operation region. (b) U as a function of α for various γ at $V = 2.4$.

4. Cut-off normalized frequency

To indicate the limit of single-mode operation the cut-off normalized frequency (V_c) of the LP_{11}-mode [5] is given in Fig. 2a. The cut-off value increases as α decreases. The numerical aperature of a fibre is normally defined in terms of the maximum refractive index in the core and is therefore the same for both stepped-index and graded-index fibres having the same maximum value. However, the degree of mode confinement, and thus other factors such as bend loss and microbend loss, can be quite different in the two cases. We therefore propose a factor G defining the 'degree of guidance' of a fibre which may be thought of, for example, in terms of the number of doping (i.e. guiding) ions in a doped silica core fibre. The factor G can be used to give an approximation of the cut-off frequency of a fibre with *any* refractive-index distribution.

Let

$$V = M(2G)^{-1/2} \tag{11}$$

where

$$G = \int_0^1 \frac{\epsilon(R) - \epsilon_2}{\epsilon_1 - \epsilon_2} R\mathrm{d}R. \tag{12}$$

For a step-index fibre $G = 1/2$ and since, for this case, $V_c = 2.405$ then the value for M is the same. The cut-off value of any other profile (V_c) is then calculated from

$$V_c = \frac{2.405}{(2G)^{1/2}}. \tag{13}$$

To check Equation 13, we first consider a fibre having a graded-index distribution:

$$\begin{aligned} \epsilon(R) &= \epsilon_1(1-2\Delta R^{\alpha}), \qquad 0 \leqslant R \leqslant 1 \\ &= \epsilon_1(1-2\Delta) = \epsilon_2 \quad R \geqslant 1 \end{aligned} \tag{14}$$

From Equations 12 and 13, we get

$$V_c = 2.405[(\alpha+2)/\alpha]^{1/2} \tag{15}$$

which is exactly the same as the approximate value obtained from the variational method [11]. In the case of a fibre having a dip, we obtain

$$V_c = 2.405\left[\frac{(\alpha+1)(\alpha+2)}{\alpha^2+3\alpha+2(1-\gamma)}\right]^{1/2}. \tag{16}$$

The comparison with the exact value is shown in Table I and II. The error becomes bigger for smaller values of α. Nevertheless, the error is within 5%. Therefore Equation 13 can give a reasonable estimate of the cut-off frequency in any kind of fibre.

5. Near-field and far-field patterns

The near-field intensity distribution can be easily determined once U is known for a fixed V. Fig. 3a shows the near-field pattern for $V = 2.4$ and $\gamma = 1$, as a function of α. It is seen that the maximum mode energy shifts gradually from the centre towards the edge of the core with increasing degree of dip. In the case of $\alpha = 1$, it is clear that the intensity at the fibre centre is no longer a maximum and the field penetrates more into the cladding. The far-field radiation pattern can be calculated from the Fraunhofer diffraction equation giving the results shown in Fig. 3b. For convenience, the intensity distributions have been normalized. The horizontal scale ($ka \sin \phi$) denotes the normalized radiation angle. It can be seen from the figure that the radiation angle becomes smaller with decrease of α, since the field spreading in the fibre is larger at smaller α. In other words, the spot size of the HE_{11}-mode increases with increase of the degree of dip. We have reported a method for the determination of core diameter, normalized frequency and the index difference between core and cladding using only the far-field radiation [6]. This method assumes a stepped refractive index without any dip in the centre of the core. However, the

TABLE I Cut-off normalized frequency for graded-index fibre [$\epsilon(R) = \epsilon_1(1-2\Delta R^{\alpha})$ for $R \leqslant 1$, $= \epsilon_1(1-2\Delta)$ for $R \geqslant 1$]

α	Approximation	Exact value	Error (%)
1	4.17	4.38	4.9
2	3.40	3.52	3.3
4	2.95	3.00	1.8
8	2.69	2.71	0.8
∞	2.41	2.41	0.0

TABLE II Cut-off normalized frequency for fibre with dip $\{\epsilon(R) = \epsilon_1[1-2\Delta(1-R)^{\alpha}]$ for $R \leqslant 1$, $= \epsilon_1(1-2\Delta)$ for $R \geqslant 1\}$

α	Approximation	Exact value	Error (%)
1	2.95	2.80	5.1
2	2.63	2.54	3.4
4	2.49	2.44	2.0
8	2.43	2.41	0.8
∞	2.41	2.41	0.0

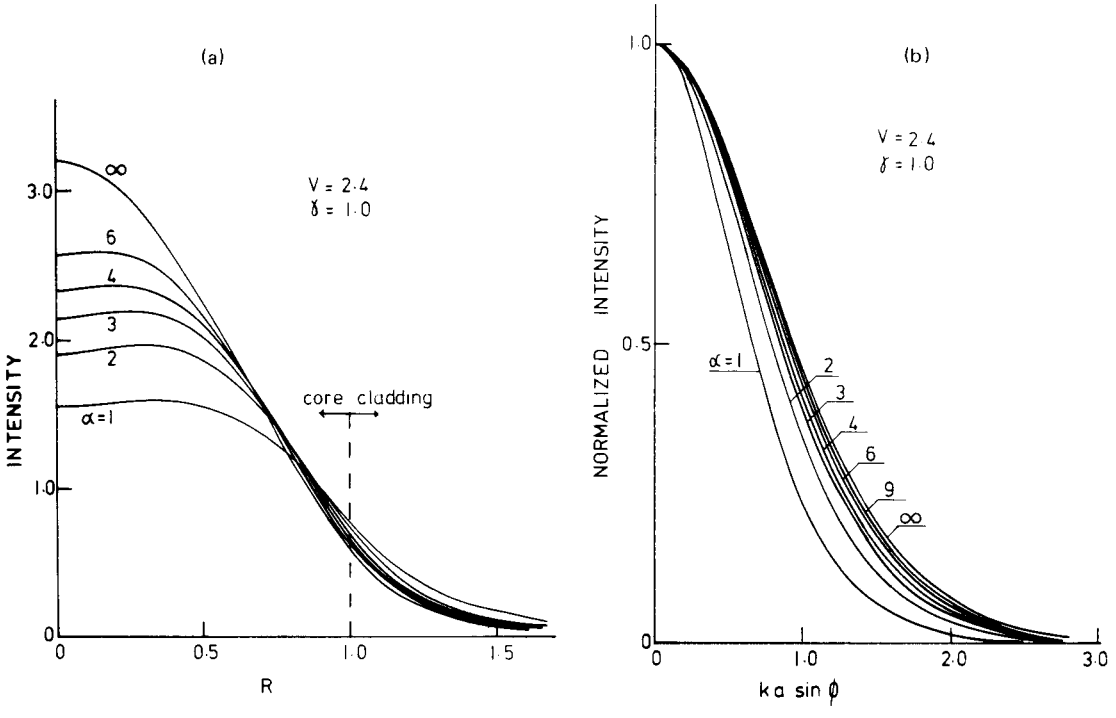

Figure 3 (a) Near-field intensity distribution of HE_{11}-mode for $V = 2.4$ and $\gamma = 1.0$ as a function of α. (b) Its far-field radiation pattern.

present results show that for $\alpha \geqslant 20$, the radiation pattern is almost the same as that of a perfect step-index fibre and the change is small for α values as small as 5. In practice [5, 6] the perturbation is within $\alpha \geqslant 20$ so that the theory of the step-index fibre is applicable.

We have so far considered the field distribution of the HE_{11}-mode in the single-mode region. However, as is expected, the influence of the dip in the refractive index on the field distribution becomes significant with increasing normalized frequency. To illustrate this tendency, the near-field and far-field patterns for $\alpha = 2$ as a function of V are shown in Figs. 4a and b, respectively, for the worst case of $\gamma = 1$. It can be seen from Fig. 4a that the field maximum shifts away from the centre of the core with increasing V. On the other hand, the intensity at the fibre centre first increases and then decreases considerably with increasing V. This suggests that the field patterns are not annular in the single-mode region, but are in the multimode region. However the far-field radiation patterns in Fig. 4b do not show any dip in the middle. The angle of radiation increases with V because of a smaller mode spot size.

From these calculations we see that the field in a single-mode region or a region containing a few modes is almost the same for $\alpha > 20$ as that of the perfect step-index fibre, but with increase of the normalized frequency the approximation only holds for larger values of α.

6. Excitation efficiency and the mode spot size

The HE_{11}-modes of step-index single-mode fibres are very nearly Gaussian in shape [3, 8]. However, as can be seen in Fig. 3a, the field is somewhat different from the Gaussian shape when a dip is present. Therefore, we must examine whether the actual HE_{11}-modal field can be still approximated by a Gaussian-shaped laser beam. First of all, the launching efficiency of the HE_{11}-mode by a Gaussian laser beam will be considered. When a TEM_{00}-beam is focused normally on a fibre core by a lens, the electric field, which is polarized in the y-direction at the focal plane ($z = 0$), can be represented by

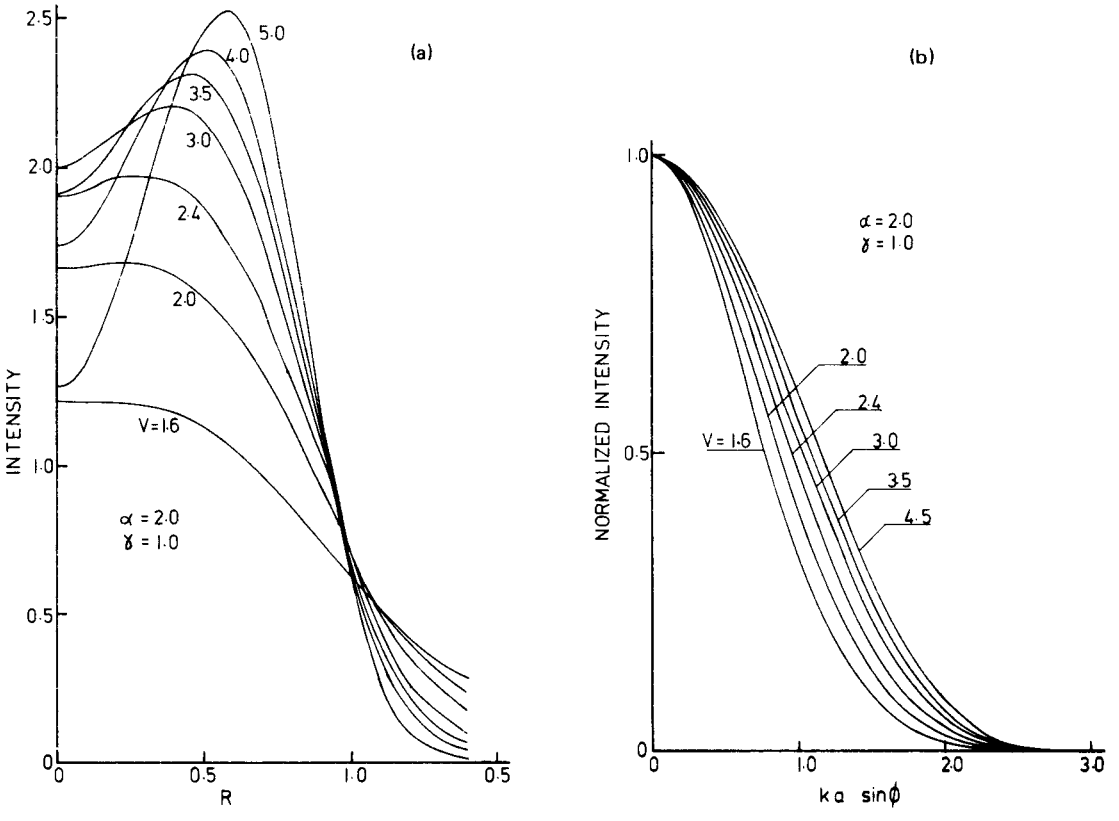

Figure 4 (a) Near-field and (b) far-field intensity distributions of HE_{11}-mode for $\alpha = 2$ and $\gamma = 1.0$ as a function of V.

$$E_y = \left[2\left(\frac{\mu_0}{\epsilon_0}\right)^{1/2} \Big/ \pi n_1 \omega_0^2\right]^{1/2} \exp\left[-\frac{1}{2}\frac{R^2}{(\omega_0/a)^2}\right] \tag{17}$$

where ω_0 is the spot size of the beam where the intensity falls to e^{-1}. With this launching condition the excitation efficiency, P, of the HE_{11}-mode is given by

$$P = \frac{4(a/\omega_0)}{\left\{2\int_0^1 \left[\frac{F(R)}{F(R=1)}\right]^2 R\mathrm{d}R + \frac{K_1^2(W)}{K_0^2(W)} - 1\right\}} \left\{\int_0^1 \frac{F(R)}{F(R=1)} \exp\left[-\frac{R^2}{2(\omega_0/a)^2}\right] R\mathrm{d}R + \int_1^\infty \frac{K_0(WR)}{K_0(W)} \exp\left[-\frac{R^2}{2(\omega_0/a)^2}\right] R\mathrm{d}R\right\}^2. \tag{18}$$

P has been evaluated numerically and is shown in Fig. 5 for the extreme case of $\alpha = 1.0$ and for $V = 2.4$. It is very important to note that the optimum input spot size changes with the depth of the dip, but that an excitation efficiency of more than 97.5% can still be achieved. This implies that the Gaussian beam is still a reasonably good approximation of the HE_{11}-mode in a single-mode fibre even with a dip in the refractive index. Therefore, the effective spot size of the HE_{11}-mode can still be defined in terms of the optimum value of ω_0 of the input Gaussian beam. Fig. 6 shows the optimum value of ω_0/a as a function of α for various normalized depths of the dip. It is shown that the spot size of the HE_{11}-mode increases for smaller values of α and larger values of γ. As stated above it is almost identical with that of the step-index fibre for $\alpha > 20$ and less than 4% different for $\alpha = 5$.

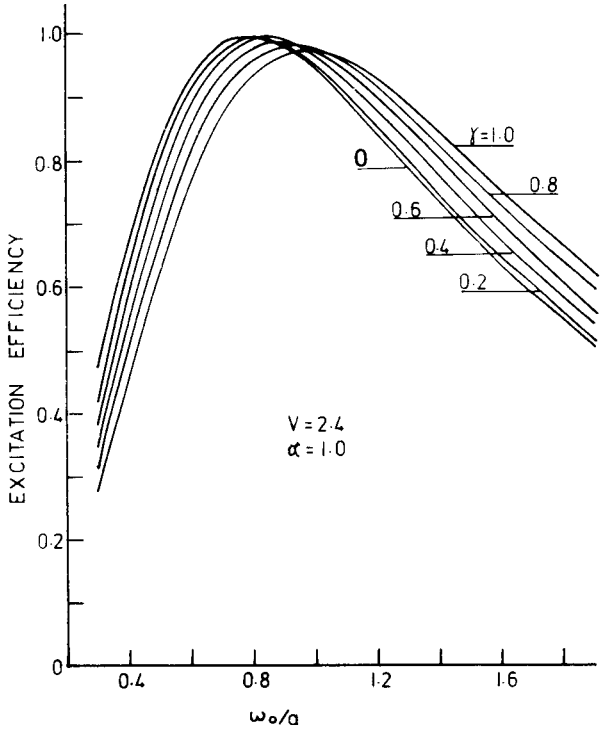

Figure 5 Excitation efficiency of the HE_{11}-mode by a Gaussian-shaped laser beam with normalized spot size (ω_0/a) for various normalized depths of the dip (γ). $V = 2.4$ and $\alpha = 1$ were used in the calculations.

As was shown in the previous section, the field distribution in the multimode region due to dip in the refractive index is apparently different from that of a perfect step-index fibre. It is, therefore, important to consider the excitation efficiency in this case. As a typical example, $\alpha = 2$ and $\gamma = 1.0$ have been chosen. The maximum value of the power transmitted is plotted as a function of V in Fig. 7, together with the optimum value of the spot size of the input Gaussian beam. At the point of interest, $V = 2.4$,

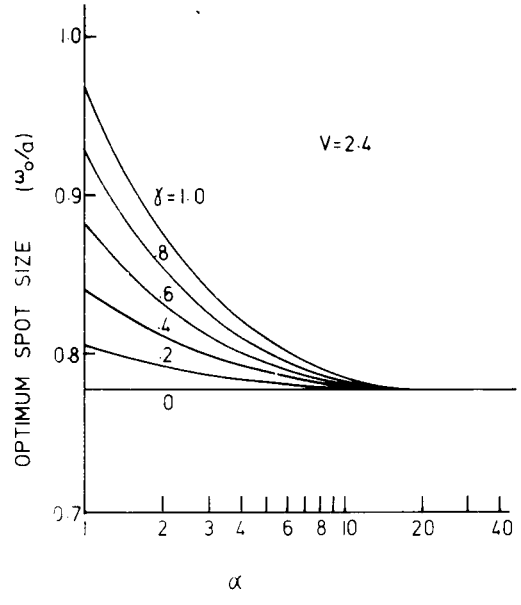

Figure 6 Normalized spot size of the HE_{11}-mode as a function of α for various γ.

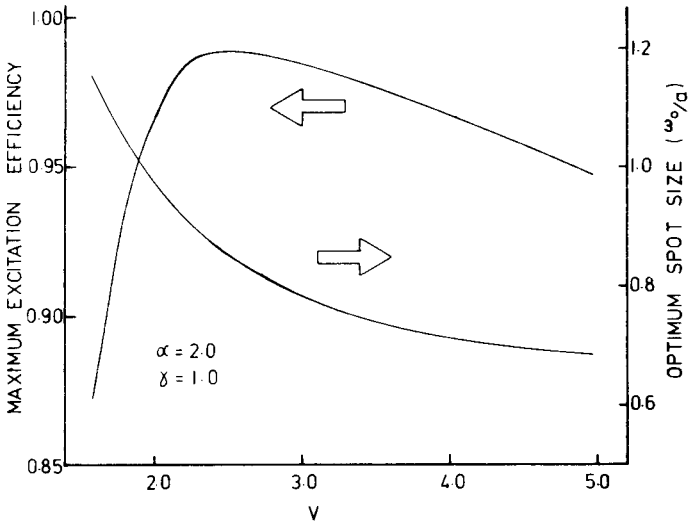

Figure 7 Maximum excitation efficiency and the optimum spot size of input Gaussian beam for $\alpha = 2$ and $\gamma = 1.0$ as a function of V.

the excitation efficiency has a maximum value. The excitation efficiency decreases very slowly for larger values of V, but for smaller V the decrease is more pronounced.

7. Conclusions

Using the weak-guidance approximation, the propagation characteristics of the HE_{11}-mode in a single-mode fibre having a dip in the refractive index have been derived analytically. Since the dip yields a smaller value for the 'degree of guidance', the energy spreads considerably from the core centre towards the edge. However, this field distribution can still be approximated by a Gaussian beam. A simple method of estimating the cut-off value in a single-mode fibre having any kind of index profile has been presented. We can conclude that if the parameter of dip (α) is greater than 20 then the propagation characteristics are almost identical with those of the step-index fibre and, in practical terms, any departure is small for α values as low as 5 even for a dip as severe as $\gamma = 1$.

Acknowledgements

Grateful acknowledgement is made to the Pirelli General Cable Company for the award of a research fellowship and to the Science Research Council for supporting the work and for a research studentship.

References

1. W. A. GAMBLING, D. N. PAYNE, C. R. HAMMOND and S. R. NORMAN, *Proc. IEE* **123** (1976) 570–6.
2. W. A. GAMBLING, D. N. PAYNE and H. MATSUMURA, *Elect. Lett.* **13** (1977) 139–40.
3. W. A. GAMBLING and H. MATSUMURA, *Opt. Quant. Elect.* **10** (1978) 31–40.
4. R. H. STOLEN, *Appl. Opt.* **14** (1975) 1533–7.
5. W. A. GAMBLING, D. N. PAYNE and H. MATSUMURA, *Elect. Lett.* **13** (1977) 174–5.
6. W. A. GAMBLING, D. N. PAYNE, H. MATSUMURA and R. B. DYOTT, *Microwaves Opt. Acoust.* **1** (1976) 13–7.
7. K. PETERMANN, *Elect. Lett.* **12** (1976) 107–9.
8. D. MARCUSE, *Bell Syst. Tech. J.* **56** (1977) 703–18.
9. W. A. GAMBLING and H. MATSUMURA, *Elect. Lett.* **13** (1977) 691–3.
10. D. GLOGE, *Bell Syst. Tech. J.* **55** (1976) 905–15.
11. K. OKAMOTO and T. OKOSHI, *IEEE Trans. Microwave Theory Tech.* **MTT-24** (1976) 416–21.